Finger-Based Personal Authentication: A Comparison of Feature-Extraction Methods Based on PCA, MDF and RD-LDA

Nikola Pavešić[1], Slobodan Ribarić[2] and Benjamin Grad[1]

[1] Faculty of Electrical Engineering, University of Ljubljana, Tržaška 25, 1000 Ljubljana, Slovenia, E-mail: Nikola.Pavesic@fe.uni-lj.si

[2] Faculty of Electrical Engineering and Computing, University of Zagreb, Unska 3, 10000 Zagreb, Croatia, E-mail: slobodan.ribaric@fer.hr

Abstract: In this paper, feature-extraction methods based on Principal Component Analysis (PCA), Most Discriminant Features (MDF), and Regularized-Direct Linear Discriminant Analysis (RD-LDA) are tested and compared in an experimental finger-based personal authentication system. The system is multimodal and based on features extracted from eight regions of the hand: four fingerprints (the prints of the finger tips) and four digitprints (the prints of the fingers between the first and third phalanges). All of the regions are extracted from one-shot grey-level images of the palmar surface of four fingers of the right hand. The identification and verification experiments were conducted on a database consisting of 1840 finger images (184 people). The experiments showed that the best results were obtained with the RD-LDA-based feature-extraction method – 99.98% correct identification for 920 tests and an Equal Error Rate (EER) of 0.01% for 64170 verification tests.

1 Introduction

The human hand provides the source for a number of physiological biometric features; among the most commonly used are the geometry of the hand [1]–[5], the dermatoglyptic patterns of the fingerprints [6]–[8] and the palmprints [9]-[11]. These features are used in both unimodal and multimodal biometric systems for user authentication. A detailed overview of the progress in this area can be found in [12]–[15].

In this paper a comparison of three appearance-based feature-extraction methods – Principal Component Analysis (PCA), Most Discriminant Features (MDF) and Regularized-Direct Linear Discriminant Analysis (RD-LDA) – is reported for an experimental finger-based authentication system based on the integration of

fingerprint (the prints of the fingertips) and digitprint (the prints of the fingers between the first and third phalanges) features. The system is a multimodal type and uses fusion at the matching-score level.

The state of the art in fingerprint recognition is extensively described in the monograph by Maltoni et al. [8]. Most fingerprint-based authentication systems follow the minutiae-based approach [16]–[17]. To overcome the sensitivity of minutiae-based approaches to the noise of the sensor and the distortion during the acquisition of the fingerprint, fingerprint-authentication systems that follow appearance-based approaches have been developed [18]–[20]. These systems also offer low error rates for fingerprint images of poor quality or for images captured by small solid-state sensors, but at a much higher computational efficiency than minutiae- and ridge-based approaches. For high-security applications, multimodal fingerprint-based systems are used [21].

Finger-based personal authentication systems are mostly based on the 2- or 3-dimensional geometry of one or two fingers. Such systems are proposed for low/medium-security environments [22]. The single-finger geometry-based biometric system [23] uses only the index finger. This finger pushes a plunger/button, which goes into the device. The rollers, which scan the finger, then take measurements of 12 cross-sections of 1½ phalanges of the finger. The two-finger geometry-based biometric system [24] uses a camera-based sensor system to take 3-dimensional measurements of the index and middle fingers. From the image a set of geometrical features of the fingers (length, width and thickness of the fingers measured on different finger sections) is extracted.

An authentication system based on the fusion of the geometry of four fingers and the dermatoglyptic patterns of four finger-strips is described in [25]. A finger-strip region is defined with respect to the finger's line of symmetry and takes an area between the first phalanx of the finger and the region of the fingerprints. The system is based on fusion at the matching-score level of the finger geometry and the PCA features extracted from the finger-strips. The experimental results, obtained on a database of 1270 images of 127 people, showed the effectiveness of the system in the sense of an EER = 1.17% and the minimum TER = 2.03% for identification.

A prototype of a biometric identification system based on fingerprint and digitprint features is presented in [26], where the fingerprint and digitprint regions of a finger

are defined in the same way as in this paper. The most discriminant features (MDF) approach is used for the feature extraction. Fusion at the matching-score level of the MDF coefficients obtained from four fingerprint and four digitprint regions is used. The experimental results, obtained on a database of 1840 images of 184 people, show the effectiveness of the system in the sense of a correct identification rate of 99.80%.

2 Description of the system

Fig.1. shows the architecture of the experimental multimodal finger-based biometric authentication system.

In the image-acquisition phase, an image of the palmar surface of the little, ring, middle, and index fingers of the right hand is taken using a small desktop scanner. Note that the thumb is not included because of its specific position related to the surface of the scanner. The spatial resolution of the images is 600 dots per inch (dpi)/256 grey levels, to adhere to the FBI standard for fingerprint images [27].

In the pre-processing module some standard image pre-processing and enhancement procedures (global thresholding, contour extraction, extraction of the relevant points on the contour) are applied. Based on the contour of four fingers and the relevant points on it, the eight regions of interest (ROIs) are localized: four strip-like rectangular regions of the fingers between the first and third phalanges, called *digitprints*, and four rectangular regions of the finger tips, called *fingerprints*. Afterwards, the ROI sub-images are cropped from the grey-scale image, rotated to the same position, sized to fixed dimensions and then light normalized.

In the subsequent eight feature-extraction modules, the extraction methods based on the PCA (for the first experiment), the MDF (for the second experiment) and the RD-LDA (for the third experiment) are used to extract the features from the normalized ROI sub-images. In the eight matching modules the matching between the live templates and the templates from a system database based on the Euclidean distance is performed. After the score normalization of the matcher's outputs, fusion based on the weighted-sum rule is applied. In the decision module the output of the fusion module is compared with the threshold, and the final decision is made (acceptance or rejection of the user's claimed identity in the case of verification, or a person's identity in the case identification).

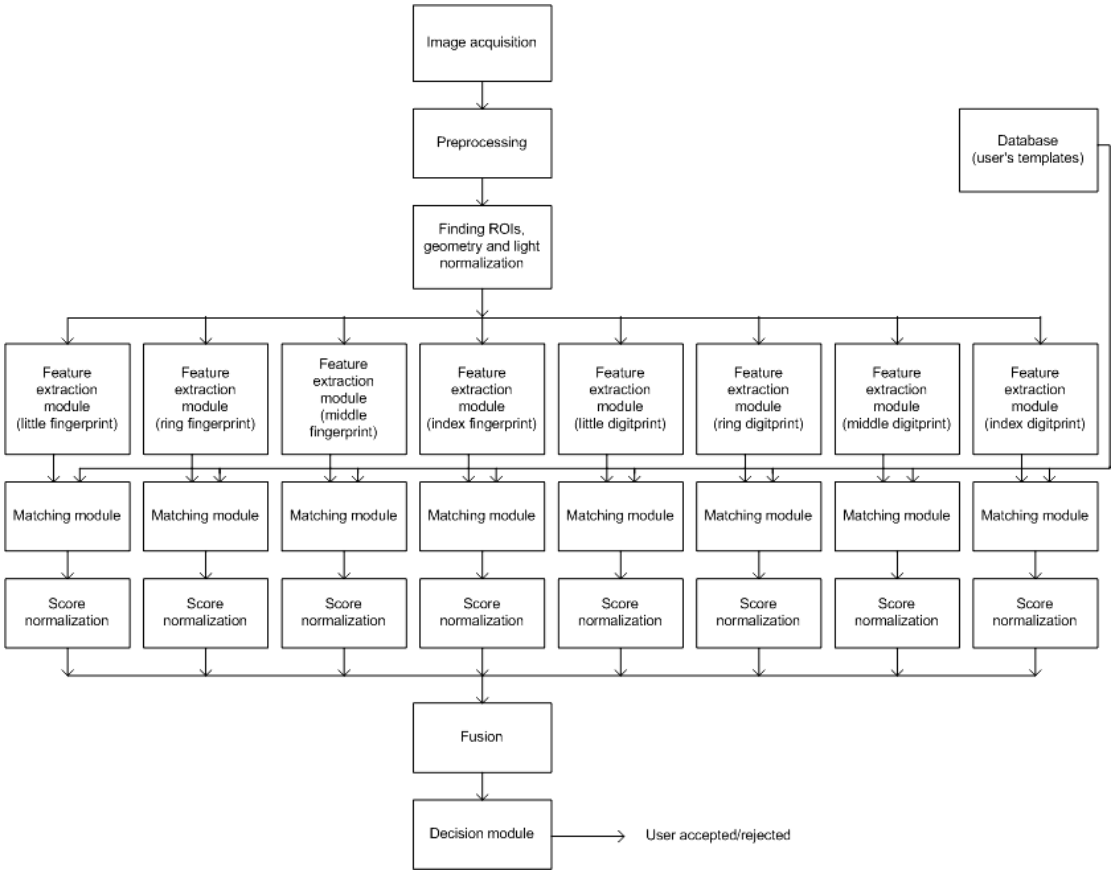

Figure 1 The architecture of the experimental multimodal finger-based authentication system

3 Image acquisition, pre-processing and normalization

3.1 Image acquisition

Images of the palmar surface of four fingers of the right hand are scanned at 600 dpi/256 grey levels using a small scanner (the dimensions of the scanning area are 15x16 cm). The user puts his/her four fingers, spread naturally, on the scanner, which has no pegs or any other hand-position constrainers.

3.2 Pre-processing

The acquired image is binarized using thresholding. Due to the controlled light conditions during the acquisition process and the high contrast between the background and the hand in the images, simple global thresholding [28] provides satisfactory results. Subsequently, by using a contour-following algorithm applied to the binary image, the contour of four fingers is extracted. The contour-following

algorithm is based on the border-following procedure for binary images described in [29]. The basic idea of the algorithm is to select the pixels of a finger (called the border pixels) that have one or more pixels in their 8-connected neighborhood belonging to the background. A pixel pair, where one pixel belongs to the finger and another is from the background, is marked with the starting label. Subsequently, in a clockwise direction, the algorithm assigns a new label index to the border pixels until the starting label is no longer met.

3.3 Localization of the finger's regions of interest

The localization of the eight regions of interest (ROIs) on the grey-scale image of the four fingers of the right hand, applied in our system, is based on the algorithm described in [14] and [30]. According to this algorithm, the localization of the ROIs is based on determining the following relevant points on the fingers' contour: T_1, T_2, T_3, and T_4 (fingertips), B_2, B_3, B_4 and B_6 (valleys between the fingers), B_1 and B_5, (additional points relevant to determining the fingers' lengths), and, finally, on each finger the points F_1, F_2, F_3 and F_4 (additional points relevant for determining the ROIs on the fingers).

The points T_1, T_2, T_3, T_4, B_2, B_3 and B_4 are located by tracking the local minima and maxima on the fingers' contour. Points B_1 and B_5 are determined so that the length of the straight line T_1–B_2 equals the length of the straight line T_1–B_1, and the length of the straight line T_4–B_4 equals the length of the straight line T_4–B_5. On the fingers' contour the points are located as shown in Fig. 2a.

On each finger, four additional, relevant points are located as follows: points F_1 and F_2 at one-third of the length of the finger, and points F_3 and F_4 at two-thirds of the length of the finger, respectively. The length of the finger is defined as the length of the straight line between the tip of the finger, T_f, and the middle-point of the straight line connecting the points B_f and B_{f+1}, where f is the index denoting the finger: $f = 1, 2, 3, 4$. The straight line connecting the middle points of the segments F_1–F_2 and F_3–F_4 defines the line of symmetry for the finger. Fig. 2b shows the contour of the ring finger, the relevant points on the contour, as well as the fingerprint and digitprint ROIs.

Based on these reference points, the ROIs on the gray-level image of the four fingers of the right hand are determined as follows:

- The digitprint ROI is a rectangle with its length chosen to be the length of the finger divided by 1.5, and its width equal to the length of the finger divided by 2.3. The rectangle is positioned on the line of symmetry, as shown in Fig. 3b.
- The fingerprint ROI is a rectangle positioned on top of the digitprint rectangle, as shown in Fig. 2b. The length of the rectangle is equal to the length of the finger divided by 2.8, and the width is equal to the length of the finger divided by 3.45.

The scanned gray-scale image with the marked contour, the relevant points and the nine regions of interest is shown in Fig. 2c.

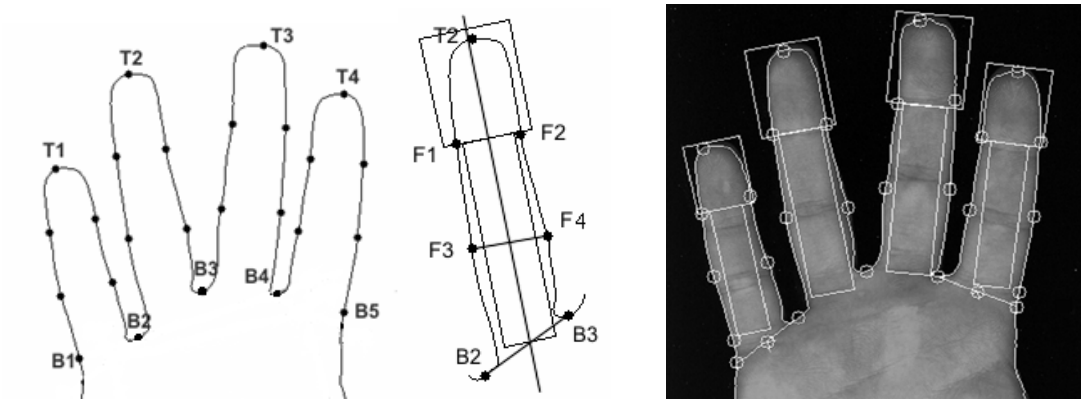

a) b) c)

Fig. 2. (a) Relevant points on the fingers' contour; (b) Relevant points on the contour of the ring finger and the fingerprint and digitprint ROIs; (c) The fingers' contour, the relevant points on the contour and the eight ROIs on the gray-scale image.

3.4 Geometry and light normalization

The ROIs in the original grey-scale images vary in size and orientation from image to image. In order to apply the feature-extraction methods (PCA, MDF and RD-LDA) the ROIs need to be normalized to exactly the same size and orientation. The ROI sub-images are cropped from the grey-scale image, rotated in such a way that all have a vertical orientation, and then sized to the fixed dimensions: the fingerprint ROI sub-images to 64 x 64 pixels, and the digitprint ROI sub-images to 16 x 64 pixels. The rotation of the cropped images and their resizing are obtained by using the functions *cv2DRotationMatrix* and *cvResize* from the *OpenCV* program library [31].

For the light normalization we used and tested two methods: histogram fitting and contrast enhancement [28]. Based on the results of the experiments we decided to perform the light normalization using the contrast-enhancement method.

4 Feature-extraction methods

The concepts of eigenspace and Fisherspace have been widely used in face and palmprint authentication [9], [32]. For experimental purposes, in our system we use the same concepts, i.e. the PCA, MDF and RD-LDA transformations of fingerprint and digitprint ROIs, to see whether they offer acceptable features for finger-based authentication when fingerprint- and digitprint-based modules are components of a multimodal biometric system.

At the features-extraction stage of the proposed system the features are generated from the ROI sub-images of the fingers by means of three appearance-based feature-extraction methods: the PCA [33] and two variants of the LDA [34] (the MDF [35] and the RD-LDA [36]), which were found to be appropriate for small numbers of training samples per class and the high dimensions of the ROI sub-images.

In the context of the fingerprint and digitprint feature-extraction problem, the PCA, LDA, MDF and RD-LDA can be formally described as follows:
Let us consider a ROI sub-image of a fingerprint or digitprint with the dimensions $k \cdot l$ pixels as a column n-dimensional vector $\vec{x}$; ($n = k \cdot l$). Each vector component represents the value of the grey-level of the corresponding pixel. Let us also assume that there is a training set L of N ROI vectors $L = \{\vec{x}_1, \vec{x}_2, \ldots, \vec{x}_N\}$. Each ROI vector $\vec{x}_k \in L$ belongs to one of c classes $\{\omega_1, \omega_2, \ldots, \omega_c\}$. Let N_i denote the number of ROI vectors in each of the classes ω_i; $i = 1,2, \ldots ,c$:

$$N = \sum_{i=1}^{c} N_i \,. \tag{1}$$

In the original n-dimensional space we can compute:

- the total scatter matrix:

$$\mathbf{S}_{\mathrm{T}} = \frac{1}{N} \sum_{k=1}^{N} (\vec{x}_k - \vec{\mu})(\vec{x}_k - \vec{\mu})^{\mathrm{T}} \,, \tag{2}$$

- the between-class scatter matrix:

$$\mathbf{S}_{\mathrm{B}} = \sum_{i=1}^{c} N_i (\vec{\mu}_i - \vec{\mu})(\vec{\mu}_i - \vec{\mu})^{\mathrm{T}} \text{ and} \tag{3}$$

- the within-class scatter matrix:

$$\mathbf{S}_{\mathrm{W}} = \sum_{i=1}^{c} \sum_{\vec{x}_k \in \omega_i} (\vec{x}_k - \vec{\mu}_i)(\vec{x}_k - \vec{\mu}_i)^{\mathrm{T}}, \tag{4}$$

where $\vec{\mu}_i$ and $\vec{\mu}$ are the mean vector of the class ω_i and the mean vector of the training set *L*, respectively.

4.1 Principal component analysis

Principal Component Analysis, also known as the Karhunen-Lóeve transform, is a widely used technique in pattern recognition to approximate the original *n*-dimensional data with a lower *m*-dimensional feature vector. It can be described as follows:

Let us define the linear mapping $\mathbf{W}$ from the original *n*-dimensional image space into *m*-dimensional feature space, where $m \leq \min\{n, N\}$, as:

$$\vec{y}_k = \mathbf{W}^{\mathrm{T}}(\vec{x}_k - \vec{\mu}). \tag{5}$$

The mapping $\mathbf{W} = \mathbf{W}_{\mathrm{PCA}}$ is chosen to maximize the determinant of the total scatter matrix of the projected samples $\vec{y}_k$, $k = 1,2,...,N$, i.e.,

$$\mathbf{W}_{\mathrm{PCA}} = \arg\max_{\mathbf{W}} \left| \mathbf{W}^{\mathrm{T}} \mathbf{S}_{\mathrm{T}} \mathbf{W} \right| = \left[\vec{w}_1 \quad \vec{w}_2 \quad \ldots \quad \vec{w}_m \right]. \tag{6}$$

$\mathbf{W}_{\mathrm{PCA}}$ is an *n* by *m* matrix whose columns are formed from the set of *m* *n*-dimensional eigenvectors $\vec{w}_i$, $i = 1,2,...,m$ of $\mathbf{S}_{\mathrm{T}}$ corresponding to the *m* largest eigenvalues. Note that the number of ROI vectors in the training set is usually less than the dimension of the image space ($N < n$) and there are only *N* meaningful eigenvectors [32].

Since the eigenvectors have the same dimension as the original images, and can be represented as $k \cdot l$ images, they are referred to as eigen-fingerprints or eigen-digitprints. The *m*-dimensional space spanned by these eigenvectors (eigen-fingerprints or eigen-digitprints) is called the eigenspace.

Fig. 3. shows examples of some eigen-fingerprints and eigen-digitprints obtained from the training set. The ordinal numbers of the eigen-digitprints or eigen-fingerprints are indicated by the index *i*.

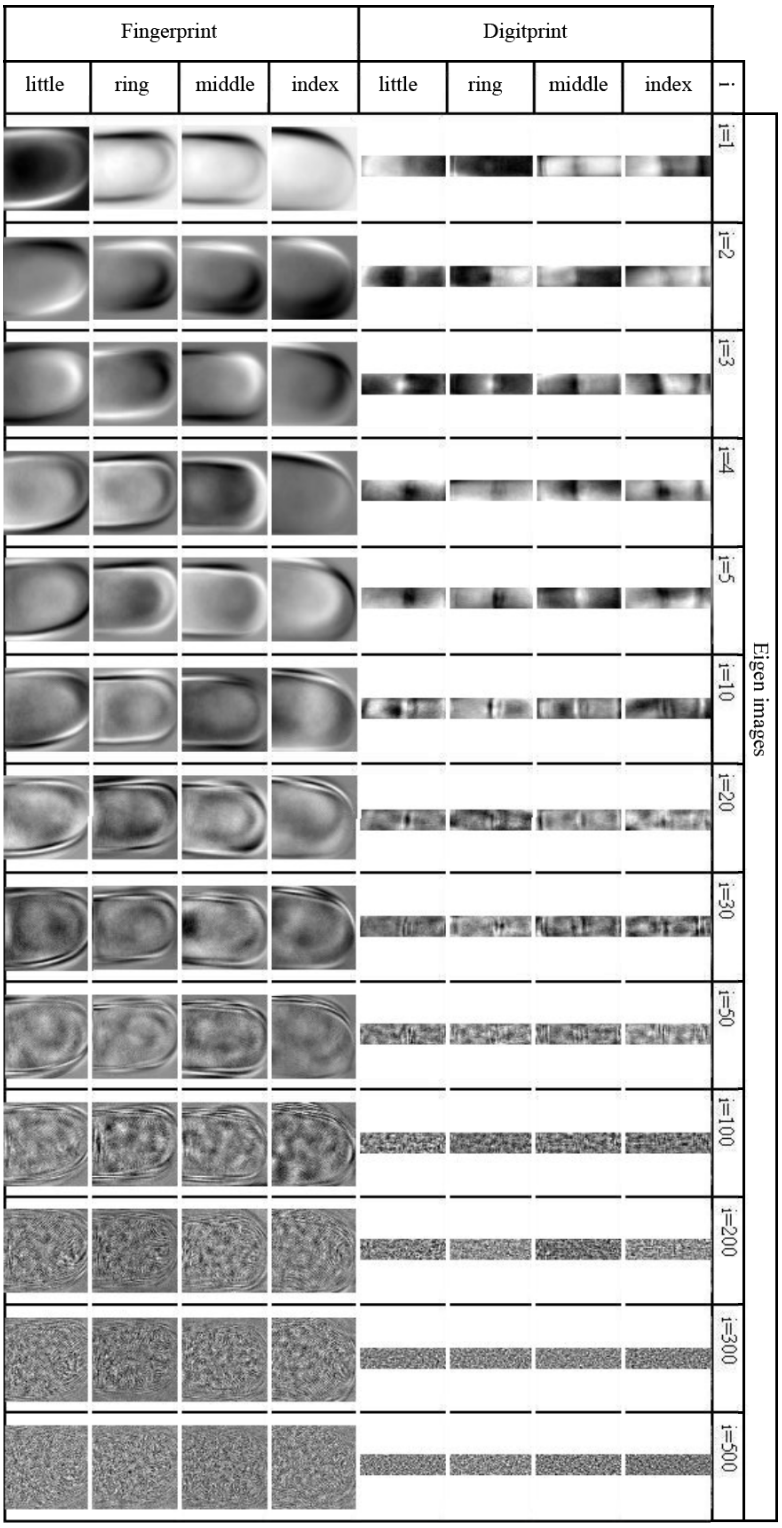

Figure 3 Eigen-fingerprints and eigen-digitprints obtained from the training set (indicated by the corresponding ordinal numbers)

4.2 Linear discriminant analysis

Linear Discriminant Analysis, also known as Fisher's Linear Discriminant (FLD), has been successfully applied in many classification problems. The LDA takes advantage of the fact that the available set of samples (the training set) is labelled and tries to find projection axes that provide the best linear separability in the transformed (feature) space. In the context of the fingerprint (digitprint) recognition problem LDA can be formally described as follows:

Let us define the linear mapping $\mathbf{W}$ from the original n-dimensional image space into the m-dimensional feature space, where $m \leq c - 1$, as:

$$\vec{y}_k = \mathbf{W}^{\mathrm{T}} \vec{x}_k. \tag{7}$$

The LDA seeks a transformation $\mathbf{W} = \mathbf{W}_{\mathrm{LDA}}$ that maximizes the ratio of the determinants of the between-class scatter and the within-class scatter matrices of the projected samples, i.e., the Fisher criterion:

$$\mathbf{W}_{\mathrm{LDA}} = \arg\max_{\mathbf{W}} \frac{\left|\mathbf{W}^{\mathrm{T}} \mathbf{S}_{\mathrm{B}} \mathbf{W}\right|}{\left|\mathbf{W}^{\mathrm{T}} \mathbf{S}_{\mathrm{W}} \mathbf{W}\right|} = \left[\vec{w}_1 \quad \vec{w}_2 \quad \ldots \quad \vec{w}_m\right] \tag{8}$$

$\mathbf{W}_{\mathrm{LDA}}$ is an n by m matrix whose columns are formed from the set of m n-dimensional eigenvectors $\vec{w}_i$, $i = 1,2,...,m$ of $\mathbf{S}_{\mathrm{W}}^{-1}\mathbf{S}_{\mathrm{B}}$ corresponding to the m largest eigenvalues. Note that the upper bound of m is $c - 1$, i.e., there are at most $c - 1$ nonzero eigenvalues.

Since the n-dimensional eigenvectors $\vec{w}_i$, $i = 1,2,...,m$ can be represented as $k \cdot l$ images, they are referred to as Fisherimages. The m-dimensional space ($m \leq c - 1$) spanned by these eigenvectors is referred to as Fisherspace.

The eigenvectors of the matrix $\mathbf{S}_{\mathrm{W}}^{-1}\mathbf{S}_{\mathrm{B}}$ can only be found in the case that the within-class scatter matrix $\mathbf{S}_{\mathrm{W}}$ is not singular. Since in the field of biometrics the number of templates (training patterns) is limited and commonly less than the dimension of the ROI vectors $\vec{x}_k$, the matrix $\mathbf{S}_{\mathrm{W}}$ is regularly singular. To overcome this problem, we have adopted two LDA-based feature-extraction approaches: the MDF method [35] and the RD-LDA method [36].

4.2.1 Most discriminant features

Reference [35] proposes that PCA is applied first to reduce the dimension of the original n-dimensional space to an $N - c$ dimensional feature space and then to apply the LDA to reduce the dimension to $c - 1$.

According to the above-described approach the MDF seeks the transformation $\mathbf{W} = \mathbf{W}_{\mathrm{MDF}}$ that maximizes the ratio of the determinants of the transformed between-class scatter and the within-class scatter matrices of the projected samples:

$$\mathbf{W}_{\mathrm{MDF}} = \arg\max_{\mathbf{W}} \frac{\left|\mathbf{W}^{\mathrm{T}}\mathbf{S}'_{\mathrm{B}}\mathbf{W}\right|}{\left|\mathbf{W}^{\mathrm{T}}\mathbf{S}'_{\mathrm{W}}\mathbf{W}\right|}, \tag{9}$$

where the transformed scatter matrices are:

$$\mathbf{S}'_{\mathrm{W}} = \mathbf{W}_{\mathrm{PCA}}^{\mathrm{T}}\mathbf{S}_{\mathrm{W}}\mathbf{W}_{\mathrm{PCA}} \tag{10}$$

$$\mathbf{S}'_{\mathrm{B}} = \mathbf{W}_{\mathrm{PCA}}^{\mathrm{T}}\mathbf{S}_{\mathrm{B}}\mathbf{W}_{\mathrm{PCA}} \tag{11}$$

The n-dimensional column vectors of the matrix $\mathbf{W}_{\mathrm{MDF}}$ are MDF images. The m-dimensional space ($m \leq c - 1$) spanned by these eigenvectors is referred to as the MDF space.

Fig. 4. shows examples of some MDF fingerprints and MDF digitprints obtained from the training set. The ordinal numbers of the MDF fingerprints and the MDF digitprints are indicated by the index i.

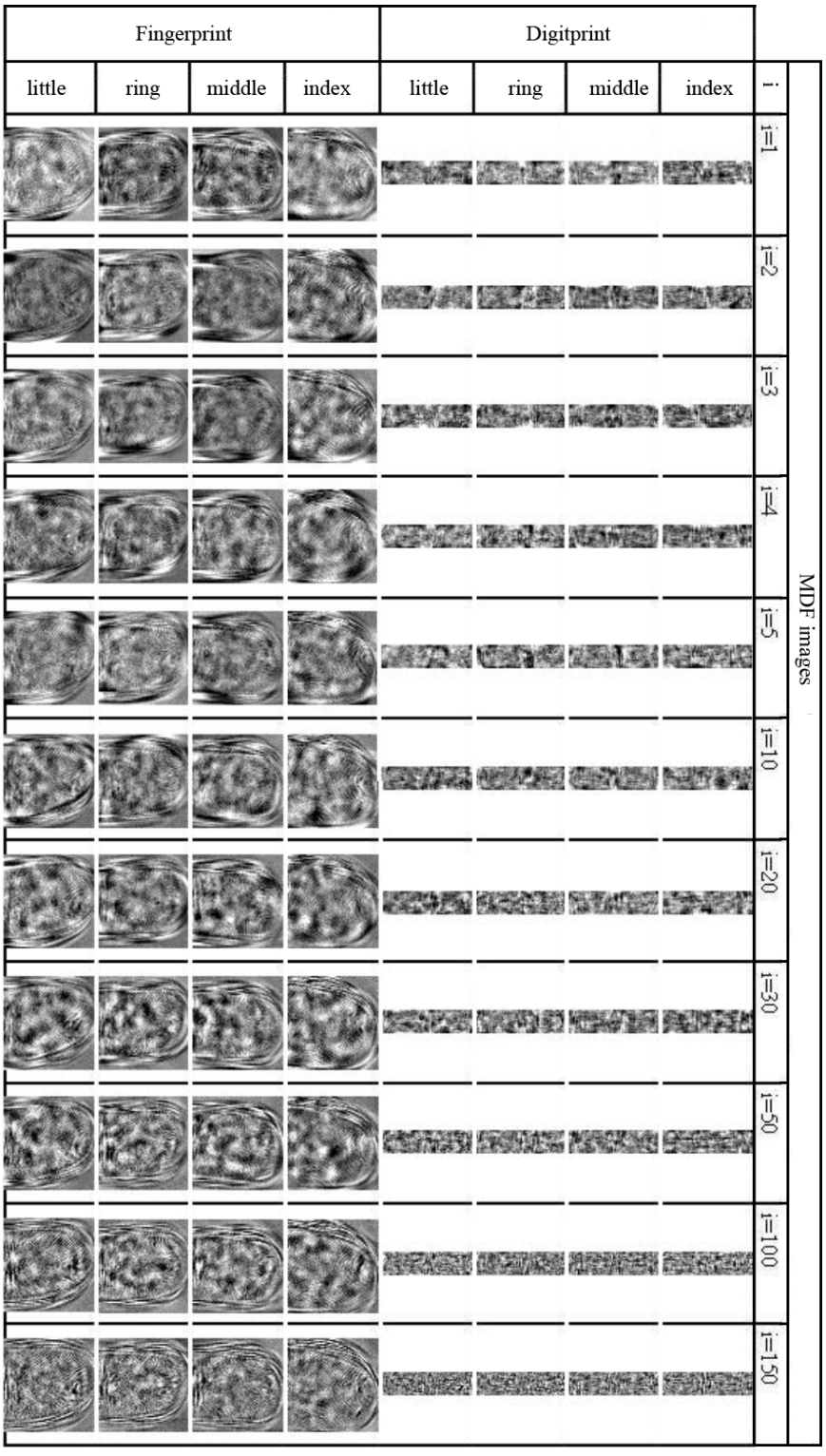

Figure 4 Examples of some MDF fingerprints and MDF digitprints obtained from the training set (indicated by the corresponding ordinal numbers)

4.2.2 Regularized-Direct Linear Discriminant Analysis

Reference [36] proposes that the transformation $\mathbf{W} = \mathbf{W}_{\text{RD-LDA}}$ is chosen to maximize the *regularized* Fisher's criterion, i.e.:

$$\mathbf{W}_{\text{RD-LDA}} = \arg\max_{\mathbf{w}} \frac{|\mathbf{W}^T\mathbf{S}_B\mathbf{W}|}{|\eta(\mathbf{W}^T\mathbf{S}_B\mathbf{W}) + (\mathbf{W}^T\mathbf{S}_W\mathbf{W})|}, \tag{12}$$

where $0 \leq \eta \leq 1$ is the parameter that controls the strength of the regularization.

The optimum value of the regularization parameter has to be determined experimentally during the system-design phase. In our case the regularization parameter η was 0.001.

Fig. 5. shows examples of some RD-LDA images: RD-Fisherfingerprints and RD-Fisherdigitprints, obtained from the training set. The ordinal numbers of the RD Fisherfingerprints and RD Fisherdigitprints are indicated by the index *i.*

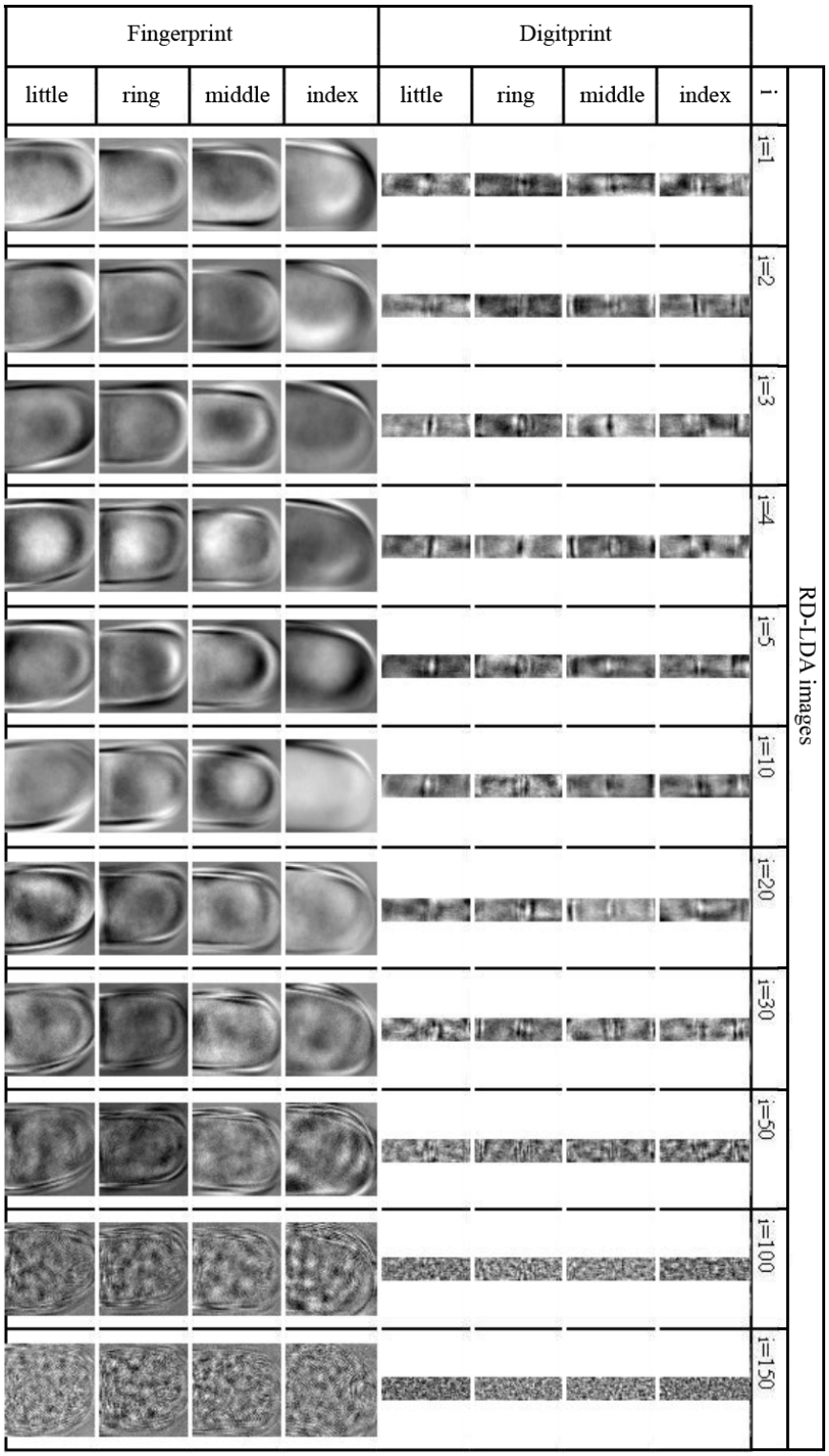

Figure 5 Examples of some RD-Fisherfingerprints and RD-Fisherdigitprints obtained from the training set (indicated by the corresponding ordinal numbers)

Due to the statistical properties of the proposed linear transformations for feature extraction, from basis images in Figures 3 – 5 is very difficult to explicitly point out the information about the salient fingerprint and digitprint features. However, we

presume that the values of the features obtained by projecting the fingerprint and digitprint images into the subspace defined by the basis images depend on regions where the singularities of the fingerprint and the digitprint are usually located (highlighted regions in the basis fingerprint and digitprint images). Note that Figures 3 - 5 depict only a (small) subset of all the used basis images.

5 Template generation, matching, normalization, fusion and decision

5.1 Template

The template, which is a mathematical representation of the biometric data for a person *p* in our system consists of eight *m*-component feature vectors: $\vec{F}_{1,p}$, $\vec{D}_{1,p}$,..., $\vec{F}_{4,p}$, $\vec{D}_{4,p}$, representing the fingerprint and the digitprint ROIs of the little, ring, middle, and index fingers, respectively. Note, that for experimental purposes, the template is generated by means of $\mathbf{W}_{PCA}$, $\mathbf{W}_{MDF}$ and $\mathbf{W}_{RD-LDA}$ (see equations (5) and (7)).

5.2 Matching

In order to identify or verify a system user, the matching process between the live template and the templates from the system database is performed using the Euclidean distance. In this step the following distances are calculated:

- $d(\vec{F}_x^i, \vec{F}_j^i)$, i = 1,2, ... 4, where $\vec{F}_x^i$ is a fingerprint live template of an unknown person x and $\vec{F}_j^i$, j = 1, 2, ... u are the fingerprint templates from the system database, where u is the total number of fingerprint (or digitprint) templates in the system database (identification) or the total number of stored templates per person (verification).

- $d(\vec{D}_x^i, \vec{D}_j^i)$, i = 1,2, ... 4, where $\vec{D}_x^i$ is a digitprint live template of an unknown person x and $\vec{D}_j^i$ are digitprint templates from the database, where j = 1, 2, ... u.

5.3 Matching-score normalization, fusion and decision

The outputs of the matching modules are normalized and transformed into similarities s_{xj}^{Fi} and s_{xj}^{Di} ; i = 1,2, ... 4, by means of eight three-linear segment functions (S^{Fi} and S^{Di} and; i = 1, 2, ... 4), which were determined experimentally from the training set [14]. The normalized outputs of the eight matching modules are combined using fusion at the matching-score level. The fusion is expressed by means of the total similarity measure (TSM_{xj}):

$$TSM_{xj} = \sum_{i=1}^{4} w_i s_{xj}^{Fi} + \sum_{i=1}^{4} w_{i+4} s_{xj}^{Di}, \quad (13)$$

where s_{xj}^{Fi} and s_{xj}^{Di} ; i=1,2,3,4 represent the corresponding values of the similarities obtained by mapping the distances into similarities. The weights w_i, i= 1,2, …8, are set proportionally to the results of the identification based on each of the finger parts obtained during the evaluation of the system; more precisely:

$$w_i = (id\_error_i)^{-1} / \sum_{i=1}^{8} id\_error_i . \quad (14)$$

In (14) id_error_i = 100 – $Average\_correct\_identification_i$, where the $Average\_correct\_identification_i$, i = 1,2, ...,8, are given in Table III.

By using the 1–NN classification rule, based on the maximum total similarity measure *TSM*, the final decision (the person's identity) is made.

6 Experiments and results

For testing purposes 10 images of the four fingers of the right hands of 184 people were acquired. The average age of the tested population (122 males and 62 females) is 36 years; the oldest is 78 years, the youngest is 21 years, all coming from the same ethnic group. To take into account the variation due to the changes between images of the same person, the images were acquired in two separate sessions over a period of three months.

In the collected database consisting of 1840 four-fingers images (184 image classes, 10 images per class), two types of experiments for person authentication were performed: closed-set identification and verification.

For the closed-set identification test five images from each image class in the database were chosen randomly and used in the enrolment stage to create the client database. The remaining five images were used to test the system. The total number of attempts in the identification test was 920.

For the verification test the database was divided into two parts: 138 (i.e., 75%) classes were used for client experiments, the remaining 46 (i.e., 25%) classes were used for impostor experiments. The finger images of each class used for the client experiments were divided into two parts: five of the ten images were used in the enrolment stage to create the client database; the remaining five images were used for the testing. The client experiments were performed by comparing five test images of the 138 test classes with the corresponding class in the client database. The total number of attempts in the verification test was 64170 (690 client experiments and 63480 impostor experiments).

Table I summarizes the database setups for the identification and verification tests.

	Database (identification)	Database (verification)
Training set - clients	184 clients, 5 images / client	138 clients, 5 images / client
Test set – clients	184 clients, 5 images / client 920 attempts	138 clients, 5 images / client 138×5 = 690 attempts
Test set – impostors	0	46 impostors 10 images / client 138×10×46 = 63480 attempts

Table I Database setups for the identification and verification tests

With the exception of the identification test in Experiment 1, which was performed only once, all the other tests were repeated 10 times, and every time another five images of four fingers where chosen randomly for the client database.

6.1. Identification experiments

6.1.1 Experiment 1: Looking for the optimal number of PCA coefficients

In order to find the optimal number of PCA coefficients for a description of the finger's ROIs the identification test was performed with 10-, 20-, 30-, 50-, 100-, 200-, 300-, 500- and 920-dimensional feature vectors. Table II displays the results of the identification tests.

With reference to the results summarized in Table II, the first 100 PCA coefficients are chosen as features representing the four fingerprint ROIs and the four digitprint ROIs in the subsequent identification and verification experiments.

ROI	PCA - Number of coefficients *m*								
	10	20	30	50	100	200	300	500	920
	Correct Identification [%]								
Fingerprint-little finger	62.5	75.2	78.1	80.3	82.5	83.2	84.1	83.8	84.0
Fingerprint-ring finger	71.9	81.0	84.3	86.2	88.1	88.3	87.8	87.8	88.6
Fingerprint-middle finger	72.2	83.1	85.5	87.4	88.8	89.1	89.0	89.5	89.6
Fingerprint-index finger	67.8	80.2	82.0	84.6	86.7	87.3	87.6	87.5	87.9
Digitprint-little finger	80.5	91.5	93.8	94.9	95.5	95.2	94.1	94.0	94.1
Digitprint-ring finger	82.0	91.1	93.7	94.8	95.1	95.1	94.9	94.8	94.9
Digitprint-middle finger	82.9	92.6	94.9	95.6	96.0	95.8	95.5	95.7	95.8
Digitprint-index finger	80.5	90.7	93.5	94.6	94.8	94.8	94.9	95.0	95.0
Fusion-all ROIs	98.8	99.1	99.2	99.2	**99.3**	99.3	99.3	99.3	99.3

Table II Rates of correct identifications based on *m*-dimensional PCA-based feature vectors representing the four fingerprint ROIs, the four digitprint ROIs and their fusion at the matching-score level

6.1.2 Experiment 2: Comparison of PCA, MDF and RD-LDA

The identification tests were performed with the following dimensions of the ROI feature vectors: the first 100 PCA coefficients, the 183 MDF coefficients (based on (N-c) = 736 PCA coefficients), the 183 MDF coefficients (based on c = 184 PCA

coefficients) and the 183 RD-LDA coefficients. The results are summarized in Table III.

ROI	Feature-Extraction Method			
	PCA m =100	**MDF** m =183 (based on $N - c$ = 734PCA coefficients)	**MDF** m =183 (based on c = 184 PCA coefficients)	**RD-LDA** m =183
	Average correct identification [%]; Standard deviation [%]			
Fingerprint-little finger	83.11; 0.82	76.30; 0.81	88.44; 0.69	91.58; 0.49
Fingerprint-ring finger	88.48; 0.78	88.58; 0.64	95.65; 0.56	96.41; 0.41
Fingerprint-middle finger	91.08; 0.62	89.13; 0.58	95.23; 0.58	96.78; 0.40
Fingerprint-index finger	90.11; 0.71	85.87; 0.68	91.41; 0.62	96.52; 0.42
Digitprint-little finger	94.82; 0.58	94.34; 0.47	94.46; 0.52	97.28; 0.36
Digitprint-ring finger	96.41; 0.50	95.43; 0.51	95.86; 0.48	98.14; 0.34
Digitprint-middle finger	96.95; 0.49	97.29; 0.38	96.96; 0.42	99.01; 0.24
Digitprint-index finger	95.65; 0.62	95.91; 0.48	95.43; 0.49	98.62; 0.26
Fusion-all ROIs	99.50; 0.43	99.78; 0.24	99.67; 0.30	99.98; 0.05

Table III Rates of the average correct identification for the three tested feature-extraction methods for the four fingerprint ROIs, the four digitprint ROIs and their fusion at the matching-score level

In Table III, the rates of the average correct identification for four-fingerprint ROIs and four-digitprint ROIs are obtained by using the 1-NN classification rule to classify the live templates $\vec{F}_x^i$ and $\vec{D}_x^i$, based on the similarities s_{xj}^{Fi} and s_{xj}^{Di}, separately for each fingerprint ROI and each digitprint ROI.

6.2. Verification experiments

6.2.1 Experiment 3: Comparison of PCA, MDF and RD-LDA

The verification test was performed with the following dimensions of the ROI feature vectors: the first 100 PCA coefficients, the 183 MDF coefficients (based on 184 PCA coefficients) and the 183 RD-LDA coefficients. Figures 6–8 show the dependency of the FAR and FRR on the threshold of the system for the PCA-, MDF- and RD-LDA-based feature-extraction methods, respectively.

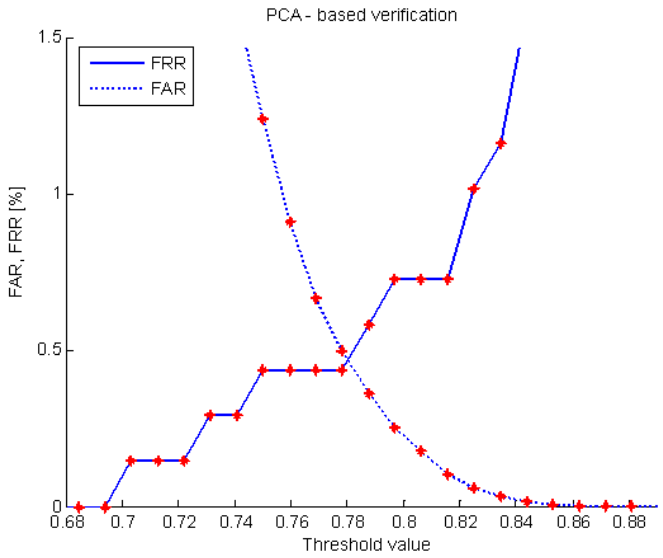

Figure 6 Verification test for the PCA-based system: plots of the dependency of the FAR and FRR on the threshold (average result of 10 repeated verification tests)

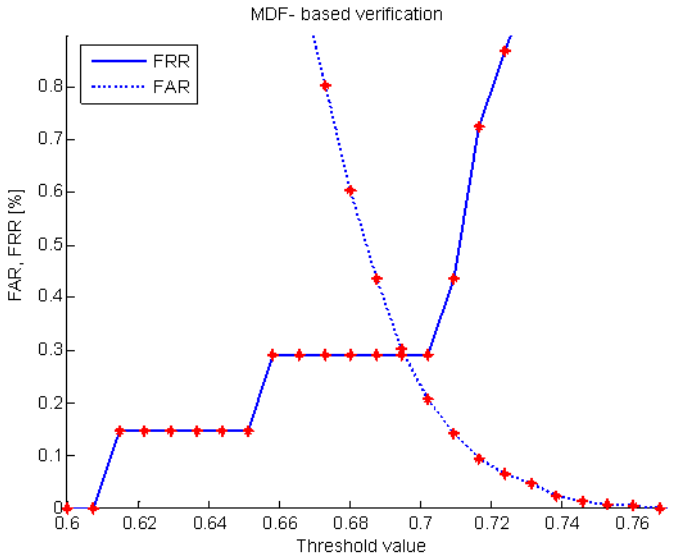

Figure 7 Verification test for the MDF-based system: plots of the dependency of the FAR and FRR on the threshold (average result of 10 repeated verification tests)

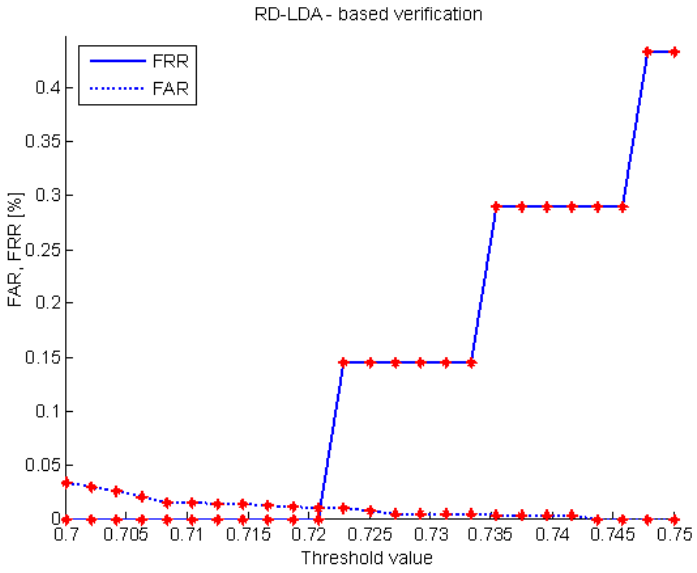

Figure 8 Verification test for the RD-LDA-based system: plots of the dependency of the FAR and FRR on the threshold (average result of 10 repeated verification tests)

From Figures 6–8 it is clear that the lowest EER = 0.01% can be achieved for the RD-LDA-based system at the threshold 0.721.

The verification-system receiver-operating curves (ROCs) for the three tested feature-extraction methods are shown in Fig. 9.

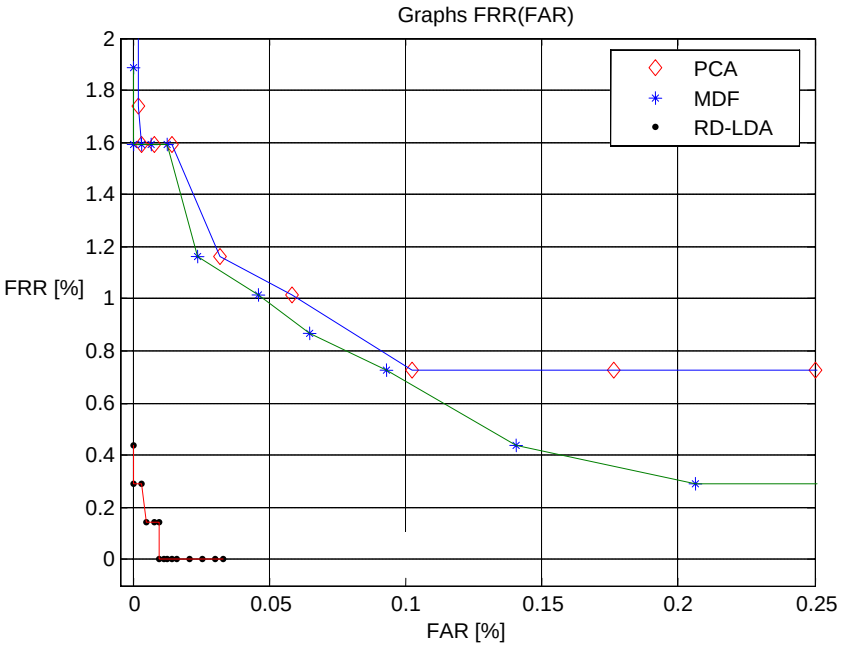

Figure 9 Verification-system receiver-operating curves (ROCs) for the three tested feature-extraction methods (average result of 10 repeated verification tests)

7 Conclusions

In this paper, feature-extraction methods based on Principal Component Analysis (PCA), Most Discriminant Features (MDF), and Regularized-Direct Linear Discriminant Analysis (RD-LDA) are tested and compared in an experimental personal authentication system based on four fingers. The identification and verification experiments showed that the best results were obtained with the RD-LDA-based feature-extraction approach (99.98% correct for 920 identification tests and an EER = 0.01% for 64170 verification tests).

The results of the correct identification rate, as well as the results of the verification, have encouraged us to continue with our research and develop a multimodal finger-based system that can be used in medium or even in high-security environments.

Since the images of the palmar surface of the fingers are usually obtained with different skin conditions (e.g., dry, wet, soiled, abraded, etc.), in the future we plan to expand our system with modules for testing the quality of the ROI sub-images and to empirically evaluate the effect of poor-quality ROI sub-images on the accuracy of the system.

8 Acknowledgements

This work has been supported by the Slovenian Ministry of Higher Education, Science and Technology, as part of the research programme Metrology and Biometric Systems, and by the Croatian Ministry of Science, Education and Sports, as part of the scientific project Theory, Modelling and Applying of Autonomy Oriented Computing Structures. The research presented in the paper is also motivated by the authors' activity within the COST Action 2101 Biometrics for Identity Documents and Smart Cards.

9 References

[1] Golfarelli M., Maio D., and Maltoni D., "On the Error-Reject Trade-Off in Biometric Verification Systems", *IEEE Trans. on the PAMI*, 19, (7), 1997, pp. 786-796

[2] Jain A. K., Ross A., and Pankanti S., "A Prototype Hand Geometry-based Verification System", *2nd Int. Conference on Audio- and Video-based Personal Authentication (AVBPA)*, Washington, March 1999, pp. 166-171

[3] Sanchez-Reillo R., Sanchez-Avila C., and Gonzalez-Marcos A., "Biometric Identification Through Hand Geometry Measurements", *IEEE Trans. on PAMI*, 22, (10), 2000, pp. 1168-1171,

[4] Zhang D. D., Automated Biometrics, Technologies and Systems, (Kluwer Academic Publishers, Boston, 2000)

[5] Jain A. K., R. Bolle, and S. Pankanti, Biometrics, Personal Identification in Networked Society, (Kluwer Academic Publishers, Norwell, 1999)

[6] Bolle R.M., Connell J. H., Pankanti S., Ratha N. K., and Senior A. W., "Guide to Biometrics", (Springer-Verlag, New York, 2004)

[7] Jain A. K., Pankanti S., and Bolle R., "An Identity-Authentication System Using Fingerprints", *Proceedings of the IEEE,* 85, (9), 1997, pp.1365-1388

[8] Maltoni D., Maio D., Jain A. K., and Prabhakar S., "*Handbook of Fingerprint Recognition"*, (Springer-Verlag, New York, 2003)

[9] Zhang D. D., "*Palmprint Authentication"*, (Kluwer Academic Publishers, Norwell, 2004)

[10] Kumar A., and Zhang D., "Personal Authentication Using Multiple Palmprint Representation", *Pattern Recognition,* 38, (10), 2005, pp. 1695-1704

[11] Rowe R. K., Uludag U., Demirkus M., Parthasaradhi and Jain A. K., "A Multispectral Whole—hand Biometric Authentication System", *Proceedings of Biometric Symposium, Biometric Consortium Conference,* Baltimore, Sep. 2007.

[12] Pavešić N., Ribarić S., and Ribarić D., "Personal Authentication Using Hand-geometry and Palmprint Features - the State of the Art", *Biometrics: Challenges arising from theory to practice*, Cambridge, 2004, pp. 17-26

[13] Pavešić N., Savič T., Ribarić S., and Fratrić I., "A Multimodal Hand-based Verification System with an Aliveness-detection Module". *Annales des télécommunications,* 62, (1/2), 2007, pp. 130-155

[14] Ribarić S., and Fratrić I., "A Biometric Identification System Based on Eigenpalm and Eigenfinger Features", *IEEE Transactions on Pattern Analysis and Machine Intelligence*, 27, (11), 2005, pp. 1698-1709

[15] Ribarić S., Ribarić D., and Pavešić N., "Multimodal Biometric User identification

System for Network-based Applications", *IEE, Proceedings on Vision, Image, Signal Processing,* 150, (6), 2003 , pp.409-416

[16] Ratha N., Karu K., Chen K., S., and Jain A. K., "A Real-time Matching System for Large Fingerprint Databases", *IEEE Transactions on Pattern Analysis and Machine Intelligence*, 18, (8), 1996, pp. 799-813

[17] Jain A., Hong K., L., and Bolle R., "On-line Fingerprint Verification", *IEEE Transactions on Pattern Analysis and Machine Intelligence*, 19, (4), 1997, pp. 302-314

[18] Tico M., Immonen E., Ramo P., Kuosmanen P., and Saarinen J., "Fingerprint Recognition Using Wavelet Features", *Proceedings of the IEEE Int. Symposium on Systems and Circuits ISCAS 2001,* Sydney, May 6-9, 2001, pp. 21-24

[19] Lee C. J., and Wang S. D., "Fingerprint Feature Extraction Using Gabor Filters", *Electronic Letters,* 35, Feb.1999, pp. 288-290

[20] Jin A. T. B., Ling D. N. C., and Song O. T., "An Efficient Fingerprint Verification System Using Integrated Wavelet and Fourier-Mellin Invariant Transform", *Image and Vision Computing,* 22, Jan. 2004, pp. 503-513

[21] Prabhakar S., and Jain A. K., "Decision-level fusion in fingerprint verification", *Pattern Recognition*, 35, (4), April 2002, pp. 861-874

[22] Vacca J. R., "*Biometric Technologies and Verification Systems"*, (Elsevier, Amsterdam, 2007)

[23] BioMet Partners Inc., http://www.biomet.ch/ accessed August 2008

[24] BioMet Partners Inc.,"Important Advantages of Biomet's Technology", 2006, http://www.biomet.h/overview.htm; Accessed December 2008.

[25] Ribarić S., and Fratrić I., "An Online Biometric Authentication System Based on Eigenfingers and Finger-Geometry", *Proceedings of 13th European Signal Processing Conference,*Antalya, Turkey, 2005, CD ROM, (5 pages)

[26] Ribarić S., and Pavešić N., "A Finger-based Personal Identification System", Int. Conference Automatics and Informatics '07, Sofia, P*roceedings: John Atanasoff Celebration Days*, Vol. 2, 2007, pp. III/29-32

[27] "FBI, Fingerprint Identification: An Overview", 2000.

[28] Gonzalez R., and Woods C. R. E., "*Digital Image Processing"*, (Addison Wesley, Reading, Massachusetts, 1993)

[29] Rosenfeld A., and Kak A., "*Digital Picture Processing*", (Academic Press, San Diego, CA, 1982)

[30] Savič T., and Pavešić N., "Personal Recognition Based on an Image of the Palmar Surface of the Hand", *Pattern Recognition,* 40, (11), 2007, pp. 3152-3163

[31] http://sourceforge.net/projects/opencvlibrary/. Accessed December 2008.

[32] Turk M., and Pentland, A., "Eigenfaces for Recognition", J. of Cognitive Neuroscience 3, 1991, pp. 71-86

[33] Jolliffe I. T., "Principal Component Analysis" (Springer, New York, 1986)

[34] Belhumeur P.N., J.P. Hespanha, and D.J. Kriegman, "Eigenspaces vs Fisherspaces: Recognition Using Class Specific Linear Projection", *IEEE Transactions on Pattern Analysis and Machine Intelligence*, 19, (7), 1997, pp. 711-720

[35] Swets D. L., and Weng J. J., "Using Discriminant Eigenfeatures for Image Retrieval", *IEEE Transactions on Pattern Analysis and Machine Intelligence*, 18, (8), 1996, pp. 831-836

[36] Lu J., Plataniotis K.N., and Venetsanopoulos A. N., "Regularization Studies of Linear Discriminant Analysis in Small Sample Size Scenarios with Application to Face Recognition", *Pattern Recognition Letters*, 26, (2), 2005, pp. 181–191